Journal of Sound and Vibration (1998) **218**(1), 164–176
Article No. sv981814

FINITE ELEMENT ANALYSIS OF SHEAR DEFORMATION IN LAMINATED ANISOTROPIC SHELLS OF REVOLUTION

C. K. CHUN
Department of Mechanical and Controls Engineering, Sun Moon University, Chunan, Korea

AND

S. B. DONG
Department of Civil and Environmental Engineering, University of California, Los Angeles, CA 90095, *U.S.A.*

(*Received* 28 *February* 1997, *and in final form* 22 *June* 1998)

1. INTRODUCTION

The low transverse moduli in fiber-reinforced composite plates and shells manifest a greater susceptibility to transverse shear and normal deformations. As a result, the range of application of classical theory for this class of structures is abbreviated *vis à vis* those fabricated of homogeneous, isotropic materials. To extend this range, transverse shear deformation must be included as its effect on flexural behavior can be pronounced. For example, classical theory predictions of lowest flexural frequencies of vibration of laminated plates and shells can be significantly higher than the actual frequencies if appreciable shear is present. Modifications of classical theory to account for shear deformation fall within the the realm of *first-order shear deformation* (*FSD*) theories.

Various FSD theories for laminated anisotropic plates and shells have appeared in the literature, namely, references [1–6]. The essence of any FSD theory is a viable shear constitutive equation relating the shear resultants Q_1 and Q_2 to their corresponding generalized shear angles γ_{1z} and γ_{2z} through the shear rigidities Γ_{ij}'s:

$$\begin{bmatrix} Q_1 \\ Q_2 \end{bmatrix} = \begin{bmatrix} \Gamma_{55} & \Gamma_{45} \\ \Gamma_{45} & \Gamma_{44} \end{bmatrix} \begin{bmatrix} \gamma_{1z} \\ \gamma_{2z} \end{bmatrix}. \tag{1}$$

The stiffnesses Γ_{ij}'s are often expressed in terms of shear correction factors k_{ij}'s as

$$\Gamma_{55} = k_{11}^2 A_{55} \quad , \quad \Gamma_{44} = k_{22}^2 A_{44} \quad , \quad \Gamma_{45} = k_{12}^2 A_{45}, \tag{2}$$

where the A_{ij}'s are integrals of each layer's shear moduli, $Q_{55}^{(k)}$, $Q_{44}^{(k)}$, $Q_{45}^{(k)}$, over the thickness of the laminate profile, i.e.,

$$(A_{55}, A_{44}, A_{45}) = \int_z (Q_{55}^{(k)}, Q_{44}^{(k)}, Q_{45}^{(k)})\, \mathrm{d}z. \tag{3}$$

0022–460X/98/460164 + 13 $30.00/0

Historically, Reissner [7] and Mindlin [8] were the first to incorporate shear deformation in a theory for homogeneous, isotropic plates. Reissner's [7] correction factors, based on elastostatics, have values of $k_{11}^2 = k_{22}^2 = 5/6$, while those of Mindlin [8], from matching thickness-shear frequencies of infinitely long waves with those predicted by linear elasticity, are $k_{11}^2 = k_{22}^2 = \pi^2/12$. In terms of the notation of equation (2), their shear rigidities take the form of $\Gamma_{55} = \Gamma_{44} = k_{11}^2 GH$ and $\Gamma_{45} = 0$ with G as the shear modulus and H the plate thickness.

Dong and Tso [3] and Dong and Chun [6] extended Mindlin's methodology to FSD theories for laminated orthotropic shells, where the natural orthotrophy axes follow the co-ordinate lines, and laminated anisotropic shells/plates, respectively. For laminated orthotropic shells/plates, there are two distinct rigidities, Γ_{55} and Γ_{44} with $\Gamma_{45} = 0$. These rigidities are based on thickness-shear motions that are naturally polarized in two mutually orthogonal plates. For laminated anisotropic shells/plates, a fundamental dilemma occurs because of a complete absence of polarized motions in two mutually orthogonal principal planes. To work past this dilemma, Dong and Chun [6] suggested the concept of *generalized principal planes* for establishing the shear constitutive relations for laminated anisotropic shells and plates. The values of Γ_{55}, Γ_{44} and Γ_{45} were found to depend strongly upon the ratio of the transverse shear moduli in directions parallel and normal to the fiber. When the two shear rigidities are equal, the correction factors are the same as those of Mindlin, i.e., $\pi^2/12$. But when this ratio differs substantially from unity, the shear correction factors are dramatically different from the values for a homogeneous, isotropic plate. The efficacy of these shear constitutive relations was verified by Chun and Dong [9] by comparing frequencies for laminated anisotropic cylindrical shells with those based on three-dimensional elasticity.

In this letter, the essential ingredients of a conical element that incorporates shear deformation for modelling shells of revolution are described, and shear deformation effects are illustrated by finite element calculations of natural frequencies of vibration of spherical and toroidal shells. Results based on classical and FSD theories are compared. To the best of these authors' knowledge, a FSD theory conical frustum with asymmetric behavior capabilities in shells of revolution has yet to appear in the literature. Nevertheless, the finite element formulation methodology is well established, so that only the interpolations of its kinematics need to be indicated herein.

An extensive body of literature exists on finite element modelling of shells of revolution. Classical theory conical frusta are well documented; see, for example, references [10–14]. Curved elements have also appeared; see references [15, 16]. With respect to transverse shear capabilities, Tessler [17] presented a two-node conical element based on interdependent variable interpolations. This concept obviates shear locking or parasitic shear without recourse to selective reduced integration. More recently, Paramasivam and Muthiah Raj [18] presented a higher order conical element. Both Tessler and Paramasivam and Muthiah Raj restricted their attention to axisymmetrical deformation of homogeneous, isotropic shells. FSD curved elements are also available for axisymmetrically loaded homogeneous, isotropic shells; see references [19–21]. Other element formulations for the analysis

of laminated anisotropic axisymmetric shells include those by Noor and Peters [22–24] (a curved element using a mixed finite element formulation) and Panda and Natarajan [25] (a superparametric element). Both of these elements possess transverse shear and normal deformation effects. Although not exhaustive, these references should illustrate the wealth of research invested in the modelling of shells of revolution.

2. FINITE ELEMENT DISPLACEMENT FIELDS

Consider a conical frustum, as shown in Figure 1, whose semi-vertex angle is α. Let (s, θ, z) be surface and normal co-ordinates and let t denote time. Let (u_s, u_θ, u_z) be the reference surface displacements in the (s, θ, z) directions, respectively, and let (β_s, β_θ) be the bending rotations about the two reference surface axes. The basic equations of FSD theory for laminated anisotropic shells/plate are contained in Dong and Chun [6]. For the conical frustum, whose

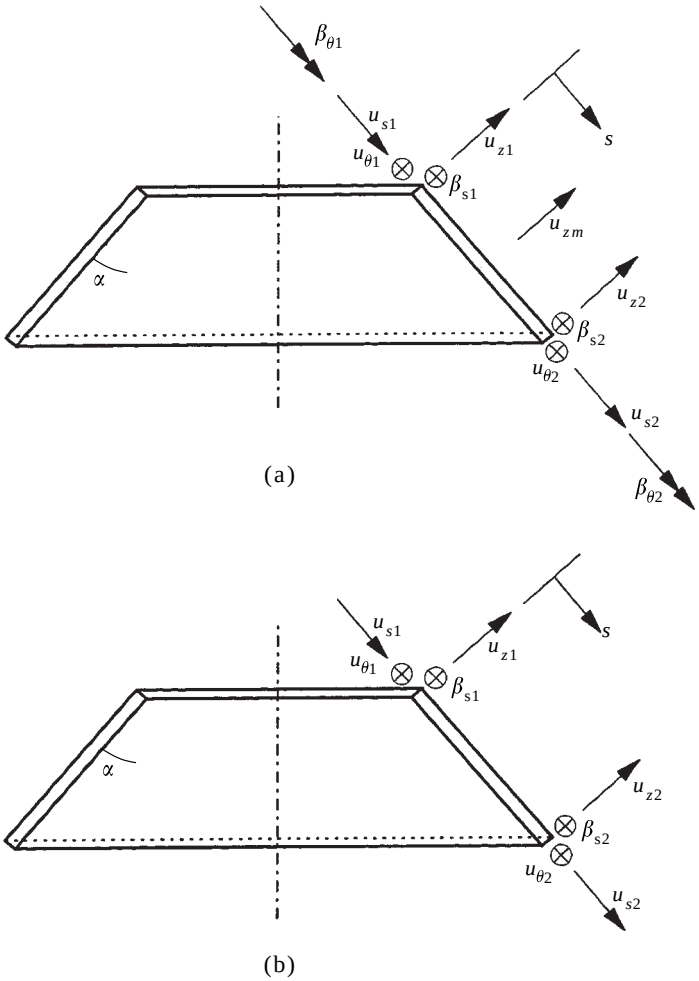

Figure 1. Nodal degrees of freedom for elements: (a) FSD theory, (b) classical theory.

nodal degrees of freedom are labelled in Figure 1, the interpolation of these five kinematic variables takes the form

$$\begin{bmatrix} u_s(s,\theta,t) \\ u_\theta(s,\theta,t) \\ u_z(s,\theta,t) \\ \beta_s(s,\theta,t) \\ \beta_\theta(s,\theta,t) \end{bmatrix} = \begin{bmatrix} \mathbf{n}_1(s) & \cdot & \cdot & \cdot & \cdot \\ \cdot & \mathbf{n}_1(s) & \cdot & \cdot & \cdot \\ \cdot & \cdot & \mathbf{n}_2(s) & \cdot & \cdot \\ \cdot & \cdot & \cdot & \mathbf{n}_1(s) & \cdot \\ \cdot & \cdot & \cdot & \cdot & \mathbf{n}_1(s) \end{bmatrix} \begin{bmatrix} \mathbf{u}_s(\theta,t) \\ \mathbf{u}_\theta(\theta,t) \\ \mathbf{u}_z(\theta,t) \\ \beta_s(\theta,t) \\ \beta_\theta(\theta,t) \end{bmatrix} \tag{4a}$$

or

$$\mathbf{u}(s,\theta,t) = \mathbf{n}(s)\mathbf{u}_o(\theta,t), \tag{4b}$$

where $\mathbf{n}_1(s)$ and $\mathbf{n}_2(s)$ contain first and second order Lagrangian functions and the displacement array $\mathbf{u}_o$ contains the nodal degrees of freedom. The interdependent interpolation strategy of having the polynomial for the transverse displacement one order higher than that for bending rotations avoids shear locking or parasitic shear without recourse to selective reduced integration. With the polynomial for u_z one order higher than that for the rotations, kinematic freedom is mathematically admitted for the vanishing of transverse shear strains should they in fact be physically insignificant in the overall behavior. It is noted that selective reduced integration of a displacement field with the same order polynomial for transverse displacement and rotation yields the same result as interdependent interpolation, because selective reduced integration effectively extracts weighted-average values of the integrals instead of capturing the exact values that cause in shear locking. The concept of interdependent interpolations was first used by Tessler and Dong [26] for Timoshenko beam elements.

For the sake of clarity in the numerical examples, the interpolations for conical element based on classical theory are also mentioned. When shear is absent, the rotations β_s and β_θ are given by

$$\beta_s = -u_{z,s}, \qquad \beta_\theta = -\frac{1}{r}(u_{z,\theta} - \cos(\alpha)u_\theta). \tag{5}$$

Only the reference surface displacements (u_s, u_θ, u_z) require interpolations. The nodal degrees of freedom for the classical theory element are shown in Figure 1 and the interpolation field is given by

$$\begin{bmatrix} u_s(s,\theta,t) \\ u_\theta(s,\theta,t) \\ u_z(s,\theta,t) \end{bmatrix} = \begin{bmatrix} \mathbf{n}_1(s) & \cdot & \cdot & \cdot \\ \cdot & \mathbf{n}_1(s) & \cdot & \cdot \\ \cdot & \cdot & \mathbf{h}_1(s) & \cdot \\ \cdot & \cdot & \cdot & \mathbf{h}_2(s) \end{bmatrix} \begin{bmatrix} \mathbf{u}_s(\theta,t) \\ \mathbf{u}_\theta(\theta,t) \\ \mathbf{u}_z(\theta,t) \\ \beta_\theta(\theta,t) \end{bmatrix} \tag{6a}$$

or

$$\mathbf{u}(s,\theta,t) = \mathbf{n}\mathbf{u}_o(\theta,t), \tag{6b}$$

where $\mathbf{n}_1(s)$ and $\mathbf{h}_1(s)$, $\mathbf{h}_2(s)$ contain Lagrangian and Hermitian polynomials and the array $\mathbf{u}_o$ in this case contains the nodal degrees of freedom shown in Figure 1.

3. GOVERNING EQUATIONS AND SOLUTION

The finite element discretization of the shell of revolution consists of an assemblage of conical frusta linked together according to inter-element kinematic continuity. Hamilton's principle underlies the problem formulation for both FSD and classical theories. For FSD theory, the discrete equations of motion are

$$\mathbf{K}_{s1}\mathbf{Q}_s + \mathbf{K}_{s2}\mathbf{Q}_{s,\theta} - \mathbf{K}_{s3}\mathbf{Q}_{s,\theta\theta} + \mathbf{M}_s\ddot{\mathbf{Q}}_s = \mathbf{0}, \tag{7}$$

and that for classical theory are

$$\mathbf{K}_{c1}\mathbf{Q}_c + \mathbf{K}_{c2}\mathbf{Q}_{c,\theta} - \mathbf{K}_{c3}\mathbf{K}_{c,\theta\theta} + \mathbf{K}_{c4}\mathbf{Q}_{c,\theta\theta\theta} + \mathbf{K}_{c5}\mathbf{Q}_{c,\theta\theta\theta\theta} + \mathbf{M}_c\ddot{\mathbf{Q}}_c = \mathbf{0}, \tag{8}$$

where $\mathbf{K}_{si}$ and $\mathbf{K}_{ci}$ and $\mathbf{M}_s$ and $\mathbf{M}_c$ are the global stiffness and mass matrices and $\mathbf{Q}_i$ are assembled nodal degrees of freedom referred to radial, circumferential and axial directions in a common cylindrical co-ordinate system for all elements. It is noted that $\mathbf{K}_{s1}$, $\mathbf{K}_{s3}$ and $\mathbf{K}_{c1}$, $\mathbf{K}_{c3}$, $\mathbf{K}_{c5}$ are symmetric matrices, while $\mathbf{K}_{s2}$ and $\mathbf{K}_{c2}$, $\mathbf{K}_{c4}$ are antisymmetric.

The solution form for natural vibrations in both cases is

$$\mathbf{Q}_i = \mathbf{Q}_o\, \mathrm{e}^{i(n\theta + \omega t)}, \tag{9}$$

where n is a circumferential mode number, ω is the natural circular frequency, and $\mathbf{Q}_o$ denotes modal pattern. Because of circumferential periodicity, only integer values of n are admissible. Substituting this solution form into the two discrete equations of motion gives

$$([\mathbf{K}_{s1} + n^2\mathbf{K}_{s3}] + in\mathbf{K}_{s2})\mathbf{Q}_o = \omega^2\mathbf{M}_s\mathbf{Q}_o, \tag{10}$$

$$([\mathbf{K}_{c1} - n^2\mathbf{K}_{c3} + n^4\mathbf{K}_{c5}]) + i[n\mathbf{K}_{c2} - n^3\mathbf{K}_{c4}]\mathbf{Q}_o = \omega^2\mathbf{M}_c\mathbf{Q}_o. \tag{11}$$

The left-hand side matrix in both cases is Hermitian by virtue of symmetry and antisymmetry in their real and imaginary parts, respectively. With $\mathbf{M}_i$ symmetric, the algebraic eigensystems assure real eigendata. In the solution, a circumferential mode number n is assigned and a subset of the lowest squared frequencies is sought.

4. DISTRIBUTION OF ENERGIES

One way to measure shear deformation is by comparing the shear energy ratios of the various natural modes. Such a calculation can be carried out *a posteriori* to the eigensolution. Let ϕ_{nm} denote the mode shape of vibration for the mth meridional mode with the nth circumferential mode number. The squared frequency ω_{nm}^2 is given by

$$\omega_{nm}^2 = \frac{\phi_{nm}^T\mathbf{K}\phi_{nm}}{\phi_{nm}^T\mathbf{M}_i\phi_{nm}}, \tag{12}$$

where **K** denotes the left-hand sides of equations (10) and (11) for FSD and classical theories. The eigenvectors in the present calculations are mass-orthonormalized so that the denominator in equation (12) is unity.

Let **C** be the combined matrix of 3×3 submatrices of the various extensional, coupling and flexural rigidities A_{ij}'s, B_{ij}'s, and D_{ij}'s and 2×2 submatrix of shear rigidities Γ_{ij}'s in the shell/plate constitutive relation, i.e.,

$$\mathbf{C} = \begin{bmatrix} \mathbf{A} & \mathbf{B} & \cdot \\ \mathbf{B} & \mathbf{D} & \cdot \\ \cdot & \cdot & \boldsymbol{\Gamma} \end{bmatrix}. \tag{13}$$

To separate energy components in FSD theory, partition **C** as

$$\mathbf{C} = \mathbf{C}_{mem} + \mathbf{C}_{bend} + \mathbf{C}_{shear} = \begin{bmatrix} \mathbf{A} & 0{\cdot}5\mathbf{B} & \cdot \\ 0{\cdot}5\mathbf{B} & \cdot & \cdot \\ \cdot & \cdot & \cdot \end{bmatrix} + \begin{bmatrix} \cdot & 0{\cdot}5\mathbf{B} & \cdot \\ 0{\cdot}5\mathbf{B} & \mathbf{D} & \cdot \\ \cdot & \cdot & \cdot \end{bmatrix} + \begin{bmatrix} \cdot & \cdot & \cdot \\ \cdot & \cdot & \cdot \\ \cdot & & \boldsymbol{\Gamma} \end{bmatrix}. \tag{14}$$

With this partitioned form of **C** and the mass-orthonormalized eigenvectors, equation (12) can be rewritten in terms of stiffness submatrices, $\mathbf{K}_{mem}$, $\mathbf{K}_{bend}$, and $\mathbf{K}_{shear}$, that reflect the individual contributions of extension, bending and shear to the squared frequency:

$$\omega^2 = \phi_{nm}^T(\mathbf{K}_{mem} + \mathbf{K}_{bend} + \mathbf{K}_{shear})\phi_{nm}. \tag{15}$$

Expanding equation (15) gives the membrane, bending, shear energy proportions for the nth circumferential mode, respectively, as $\phi_{nm}^T\mathbf{K}_{mem}\phi_{nm}$, $\phi_{nm}^T\mathbf{K}_{bend}\phi_{nm}$, $\phi_{nm}^T\mathbf{K}_{shear}\phi_{nm}$. A similar energy decomposition for classical theory is possible; but in this case, obviously, there is no shear energy.

5. EXAMPLES

The influence of transverse shear deformation on the vibrational characteristics are illustrated for two shell geometries: (1) truncated spherical shell (Figure 2(a)) and (2) toroidal shell (Figure 2(b)). Two thickness profiles were considered; three- and four-layer regular $\pm 30^\circ$ laminate profiles with total thickness of unity. The material properties of the layers are

$$\frac{E_L}{E_T} = 20 \quad , \quad \frac{G_{LT}}{E_T} = 0{\cdot}5 \quad , \quad \frac{G_{TT}}{E_T} = \lambda\frac{G_{LT}}{E_T} \quad , \quad v_{LT} = 0{\cdot}25 \quad , \quad v_{TT} = 0{\cdot}25, \tag{16}$$

where L and T denote directions parallel and transverse to the fiber and λ represents the ratio of the transverse shear moduli of this material.

The frequencies of these shells were determined for a range of geometric parameters such as radius/thickness ratio, circumferential mode number n as well as shear moduli ratio λ. The extensional, coupling, flexural rigidities (A_{ij}'s, B_{ij}'s, D_{ij}'s) of these regular three- and four-layer laminate profiles with $\pm 30^\circ$ layup are summarized in Table 1 for the case of the total laminate thickness H

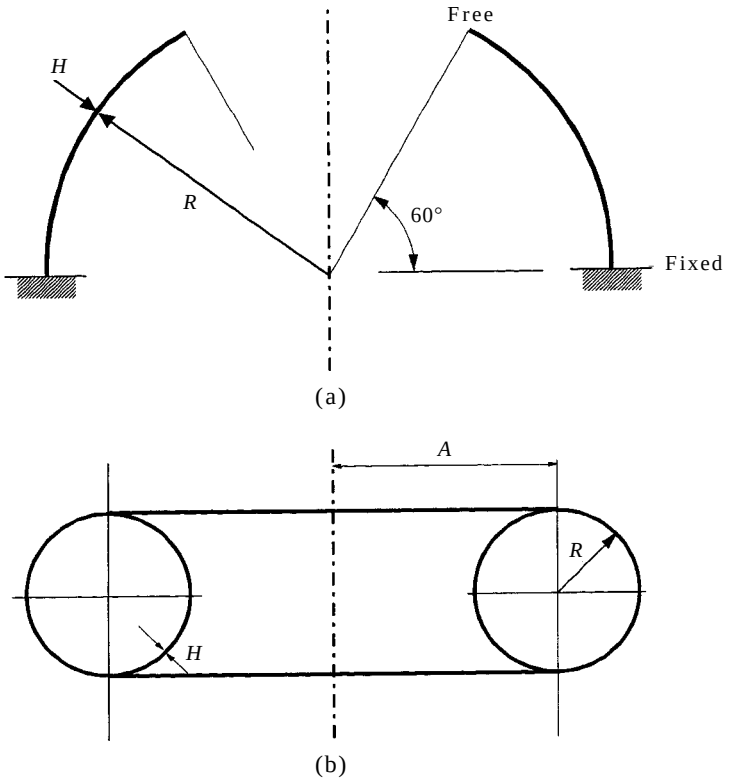

Figure 2. Shell geometries: (a) 60° truncated spherical shell, (b) toroidal shell.

equal to unity. It should also be remembered that the properties are cast with respect to given orthogonal curvilinear co-ordinates. The values of the shear rigidities, Γ_{55}, Γ_{44}, Γ_{45}, for λ ratios, $0{\cdot}1 \leqslant \lambda \leqslant 1{\cdot}0$, are tabulated in Table 2 for the total laminate thickness $H = 1$. The methodology for defining these shear rigidities was discussed by the authors [6]. It is noted that the value of λ for a typical fiber-reinforced composite falls somewhere in the range $0{\cdot}4 \leqslant \lambda \leqslant 0{\cdot}7$. For total

TABLE 1

A_{ij}, B_{ij}, D_{ij} coefficients

$ij\rightarrow$	11	12	22	66	16	26
Three-layer symmetric $\pm 30^\circ$ Laminate ($H = 1$)						
A_{ij}	11·8169	3·731548	2·287203	3·980760	2·045365	0·705618
B_{ij}	·	·	·	·	·	·
D_ij	0·984721	0·310956	0·190596	0·331733	0·473455	0·163343
Four-layer symmetric $\pm 30^\circ$ laminate ($H = 1$)						
A_{ij}	11·81701	3·731583	2·287226	3·980799	·	·
B_{ij}	·	·	·	·	−0·767020	−0·264620
D_{ij}	0·984751	0·310965	0·190602	0·331733	·	·

TABLE 2

Shear rigidities for regular $\pm 30^\circ$ *angle-ply laminates with* $H = 1$

	Three-layer laminate			Four-layer laminate		
λ	Γ_{55}	Γ_{44}	Γ_{45}	Γ_{55}	Γ_{44}	Γ_{45}
1·0	0·41123	0·41123	0·00000	0·41123	0·41123	0·0
0·9	0·40008	0·37957	−0·00387	0·40006	0·37955	0·0
0·8	0·38684	0·34620	−0·00769	0·38676	0·34611	0·0
0·7	0·37087	0·31102	−0·01135	0·37071	0·31080	0·0
0·6	0·35122	0·27392	−0·01474	0·35096	0·27349	0·0
0·5	0·32649	0·23477	−0·01764	0·32617	0·23405	0·0
0·4	0·29455	0·19343	−0·01973	0·29427	0·19236	0·0
0·3	0·25211	0·14970	−0·02045	0·25208	0·14826	0·0
0·2	0·19409	0·10332	−0·01886	0·19453	0·10161	0·0
0·1	0·11307	0·05379	−0·01316	0·11390	0·05224	0·0

laminate thickness $H \neq 1$, the values listed in Tables 1 and 2 may be scaled accordingly to give appropriate values.

5.1 *Truncated spherical shells*

In the 60° truncated spherical shell shown in Figure 2(a), clamped boundary conditions on the equatorial circle and free conditions on the 60° latitude circle

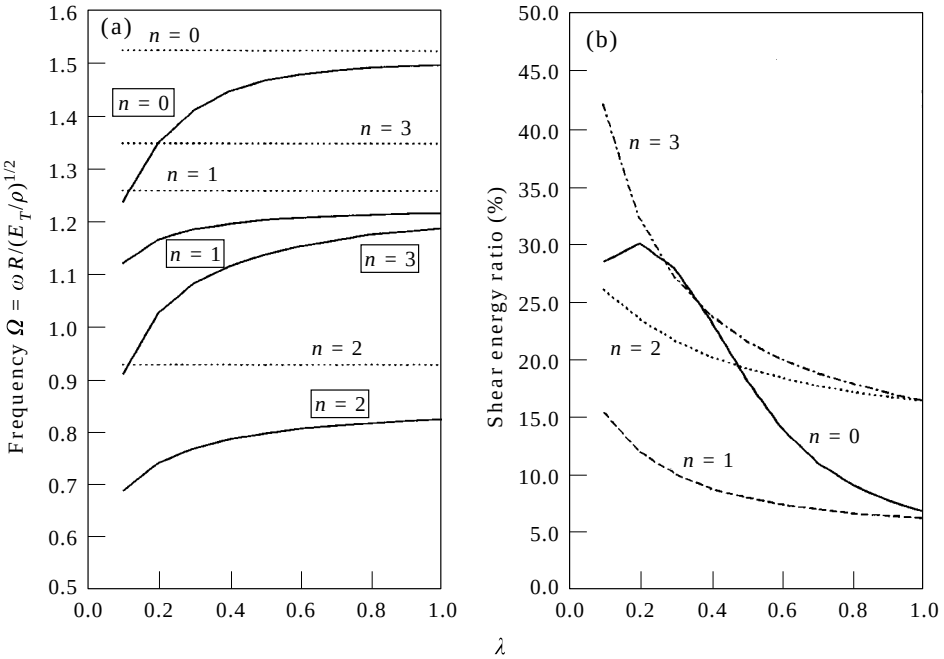

Figure 3. (a) Frequency spectra (. . . . . , classical theory; —, FSD theory) and (b) shear energy ratio in symmetric three-layer $\pm 30^\circ$ angle-ply spherical shell, $R/H = 10$: for first mode and circumferential modes, $n = 0, 1, 2, 3$.

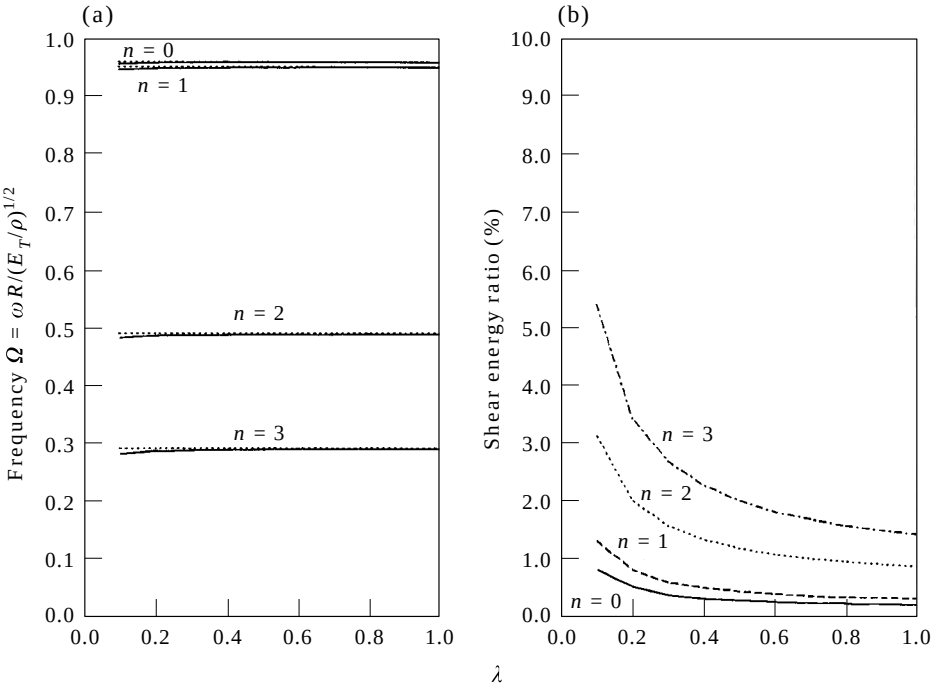

Figure 4. (a) Frequency spectra (. . . . . , classical theory; —, FSD theory) and (b) shear energy ratio in symmetric three-layer $\pm 30^\circ$ angle-ply spherical shell $R/H = 100$: for first mode and circumferential modes, $n = 0, 1, 2, 3$.

were taken. Two radius/thickness ratios, $R/H = 10$ and 100, representative of thick and thin shell geometries, respectively, were considered. The transverse shear moduli ratio λ was varied between 0·1 and 1·0. The frequencies are non-dimensionalized as $\Omega = \omega R/\sqrt{E_T/\rho}$, where ρ is the unit mass density.

Data for the regularly symmetric three-layer laminate profile are shown in Figures 3 and 4 for $R/H = 10$ and 100, respectively. In Figure 3, Ω for circumferential mode numbers, $n = 0, 1, 2, 3$, and the proportion of transverse shear strain energies in each of these modes are plotted as a function of λ. The dotted frequency curves are for classical theory results. The percentage differences between the results of the two theories reflect the levels of shear deformation. For $\lambda \to 1$, shear becomes less prominent; conversely, as $\lambda \to 0$, shear plays a greater role. Corresponding results for $R/H = 100$ (thin shell geometry) are shown in Figure 4, revealing only minor shear effects.

Data for the regularly antisymmetric four-layer laminate profile are shown in Figures 5 and 6 for the cases of $R/H = 10$ and 100, respectively. The main difference between the three- and four-layer profiles is the presence of extensional–flexural coupling through coefficients B_{16} and B_{26}. The trends observed in Figures 3 and 4 for thick and thin shell geometries are mirrored in Figures 5 and 6.

5.2 *Toroidal shells*

The toroidal shell geometry under consideration is shown in Figure 2(b). For this configuration, the studies of Kosawada *et al*. [27, 28] bear directly to our discussion. Their vibration results for homogeneous, isotropic toroidal shells showed that shear plays a minor role on the fundamental frequency (i.e., lowest mode), even though the shell geometries fall within the thick shell category (they considered R/H ratios of 9·13, 6·45 and 4·08). The explanation for this interesting and remarkable phenomenon can be explained by the fact that the fundamental mode of a toroidal shell contains membrane energy primarily, with bending (and thus transverse shear) of secondary influence. Their higher modes do in fact contain significantly more bending and transverse shear, so that these frequencies by FSD theory differ more with those of classical theory.

Let non-dimensional frequency Ω be defined in the same way as that for the spherical shell, but with R in this case as the radius of the meridional circle. In Figure 7, plots of Ω over the range $1{\cdot}5 \leqslant A/R \leqslant 10{\cdot}0$ are presented for a four-layer regular laminated composite $\pm 30^\circ$ shell. Two cases, $\lambda = 0{\cdot}5$ and $0{\cdot}1$, were considered with the former representative of a typical fiber-reinforced composite and the latter chosen to test the extent of the influence of a substantially weaker shear modulus. Plots in Figure 7(a) ($R/H = 10$) and 7(b) ($R/H = 100$) show very slight differences in the frequencies of the fundamental modes for circumferential mode numbers $n = 0$, 1, 2, 3 between those of classical and FSD theories. Even in

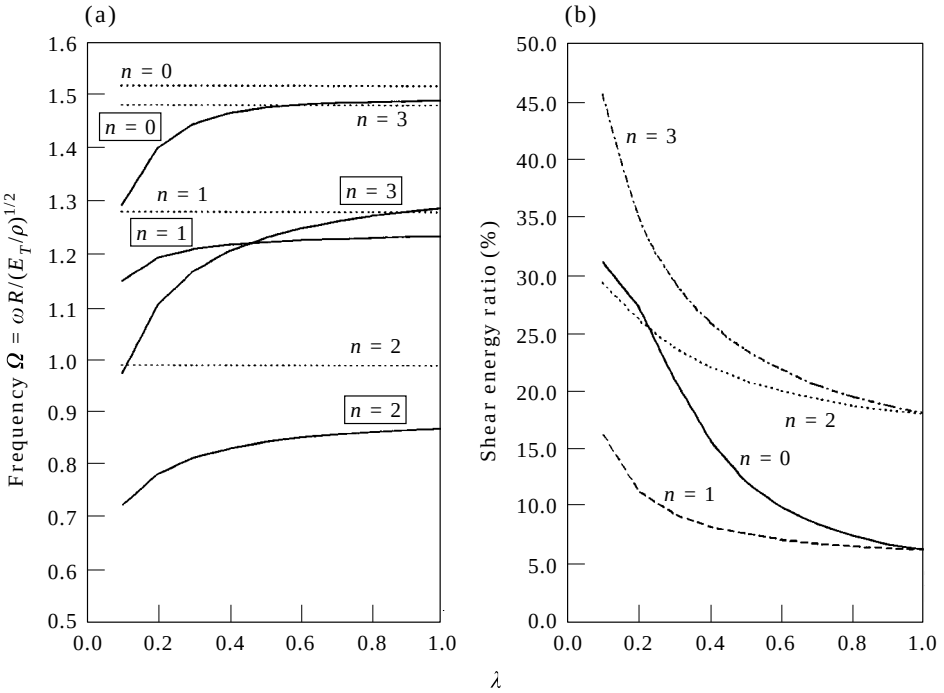

Figure 5. (a) Frequency spectra (. . . . . , classical theory; —, FSD theory) and (b) shear energy ratio in antisymmetric four-layer $\pm 30^\circ$ angle-ply spherical shell, $R/H = 10$: for first mode and circumferential modes, $n = 0$, 1, 2, 3.

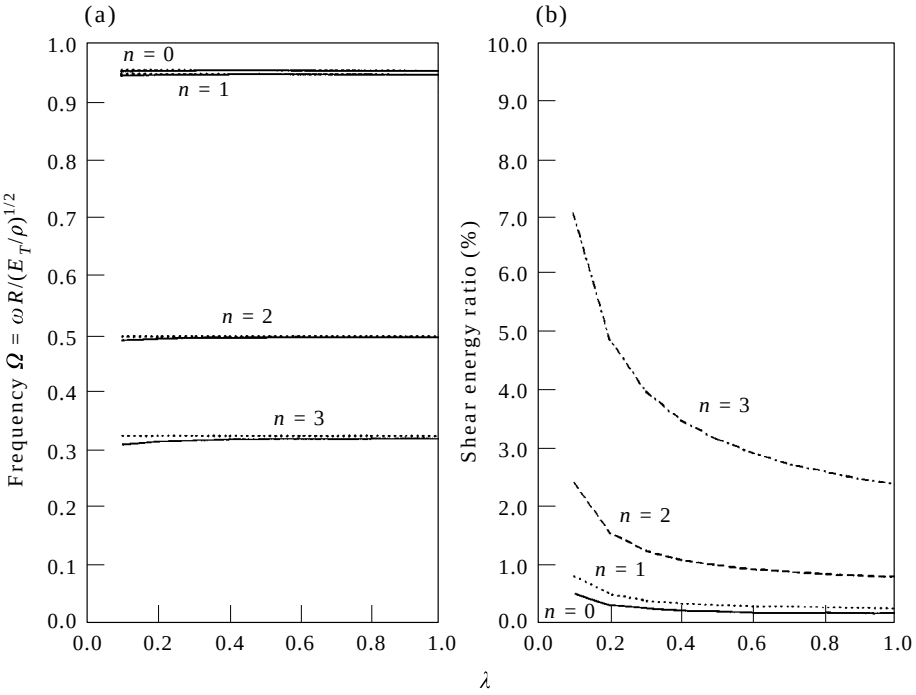

Figure 6. (a) Frequency spectra (. . . . . , classical theory; —, FSD theory) and (b) shear energy ratio in antisymmetric four-layer $\pm 30^\circ$ angle-ply spherical shell, $R/H = 100$: for first mode and circumferential modes, $n = 0, 1, 2, 3$.

the case of $\lambda = 0{\cdot}1$, the frequencies were mildly different. Therefore, the essential behavior of this laminate profile is essentially membrane, and Kosawada *et al*.'s conclusion for homogeneous, isotropic shells, also apply here for a significant orthotropy ratio $E_L/E_T = 20$. The higher modes, although not presented herein, do show wider differences in the frequencies, reflect a greater presence of transverse shear.

6. CONCLUDING REMARKS

The essence of a conical frustum shell element was presented for the axisymmetric and asymmetric analyses of laminated anisotropic shells of revolution that includes transverse shear deformation. In FSD theory, suitable transverse shear rigidities, Γ_{55}, Γ_{44}, and Γ_{45} are needed. The determination of these rigidities were discussed by the authors [6, 9] previously. The element is based on an inter-dependent displacement field interpolation, that obviates pathological shear locking without recourse to selected reduced integration. Although linear and quadratic interpolations were indicated herein, an improved element with higher order interpolations, such as that used by Paramasivam and Muthiah Raj [18], should be considered. Such capabilities would lead to comparable accuracies with substantially fewer elements in a given model.

Shear effects were evaluated by comparison of results for truncated spherical shells and toroidal shells by classical and FSD theories. The amount of transverse

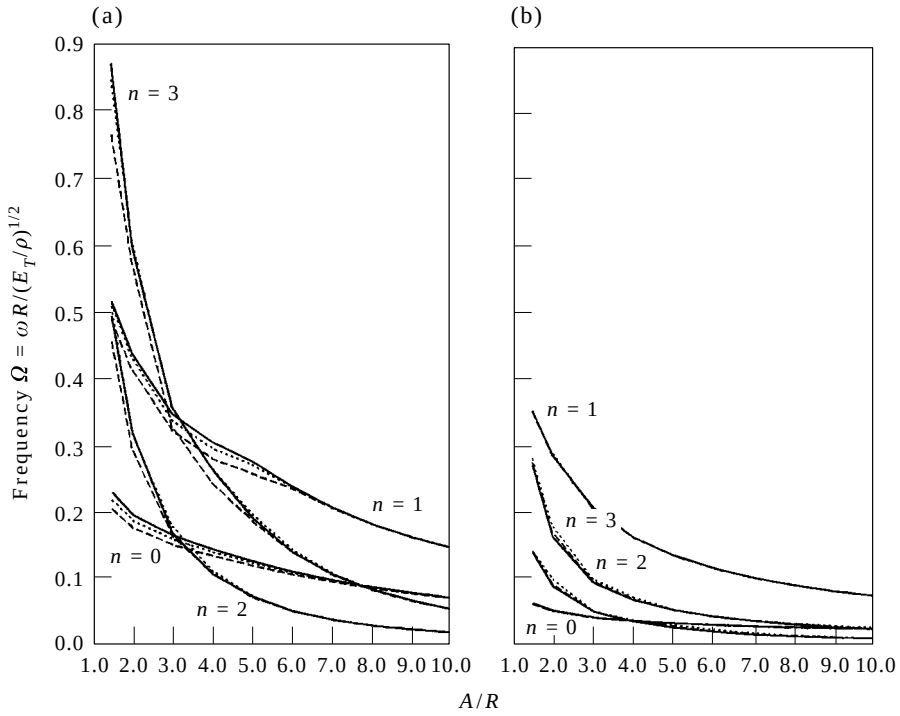

Figure 7. (a) Frequency spectra for antisymmetric four-layer $\pm 30^\circ$ angle-ply toroidal shell $R/H = 10$: for first mode and circumferential modes, $n = 0, 1, 2, 3$: (a) $R/H = 10$, (b) $R/H = 100$. —, Classical theory; . . . . , FSDT ($\lambda = 0{\cdot}5$); ---, FSDT ($\lambda = 0{\cdot}1$).

shear energy in relation to the other energies correlates directly to the differences between the frequencies of these two theories.

REFERENCES

1. P. C. Yang, C. H. Norris and Y. Stavsky 1966 *International Journal of Solids and Structures* **2**, 665–684. Elastic wave propagation in heterogeneous plates.
2. J. M. Whitney and N. J. Pagano 1970 *Journal of Applied Mechanics* **37**, 1031–1036. Shear deformation in heterogeneous anisotropic plates.
3. S. B. Dong and F. K. W. Tso 1972 *Journal of Applied Mechanics* **39**, 1091–1097. On a laminated orthotropic shell theory including transverse shear deformation.
4. E. Reissner 1972 *American Institute of Aeronautics and Astronautics Journal* **10**, 716–718. A consistent treatment of transverse shear deformations in laminated anisotropic plates.
5. E. Reissner 1979 *Computer Methods in Applied Mechanics and Engineering* **20**, 203–209. Note on the effect of transverse shear deformations in laminated anisotropic plates.
6. S. B. Dong and C. K. Chun 1992 *Journal of Applied Mechanics* **59**, 372–379. Shear constitutive relations for laminated anisotropic shells and plates: Part 1—methodology.
7. E. Reissner 1945 *Journal of Applied Mechanics*, *ASME* **47**, A69–A77. The effect of transverse shear deformation on bending of elastic plates.
8. R. D. Mindlin 1951 *Journal of Applied Mechanics* **18**, 31–38. Influence of rotatory inertia and shear on flexural motions of isotropic, elastic plates.

9. C. K. Chun and S. B. Dong 1992 *Journal of Applied Mechanics* **59**, 380–389. Shear constitutive relations for laminated anisotropic shells and plates: Part II—vibrations of composite cylinders.
10. P. E. Grafton and D. R. Strome 1963 *American Institute of Aeronautics and Astronautics Journal* **1**, 2342–2347. Analysis of axisymmetric shells by the direct stiffness method.
11. J. H. Percy, T. H. H. Pian, S. Klein and D. R. Navaratna 1965 *American Institute of Aeronautics and Astronautics Journal* **3**, 2138–2145. Application of matrix displacement method to linear elastic analysis of shells of revolution.
12. S. B. Dong 1966 *Journal of the Engineering Mechanics Division*, *ASCE* **92**, 135–155. Analysis of laminated shells of revolution.
13. S. B. Dong and L. G. Selna 1970 *Journal of Composite Materials* **4**, 2–19. Natural vibrations of laminated orthotropic shells of revolution.
14. J. Padovan 1974 *Computers and Structures* **4**, 467–483. Quasi-analytical finite element procedures for axisymmetric anisotropic shells and solids.
15. R. E. Jones and D. R. Strome 1966 *American Institute of Aeronautics and Astronautics Journal* **4**, 1519–1525. Direct stiffness method analysis of shells of revolution using curved elements.
16. I. A. Jones 1996 *Computers and Structures* **60**, 487–503. A curved laminated orthotropic axisymmetric element based upon Flügge thin shell theory.
17. A. Tessler 1982 *Computers and Structures* **15**, 567–574. An efficient conforming axisymmetric shell element including transverse shear and rotary inertia.
18. V. Paramasivam and D. Muthiah Raj 1994 *Computer Methods in Applied Mechanics and Engineering* **113**, 47–54. Shear-deformable axisymmetric conical shell element with 6-DOF and convergence of $O(h^4)$.
19. G. Prathap and C. Ramesh Babu 1986 *International Journal for Numerical Methods in Engineering* **23**, 711–723. A field consistent three-node quadratic curved axisymmetric shell element.
20. C. Ramesh Babu and G. Prathap 1986 *International Journal for Numerical Methods in Engineering* **23**, 1245–1261. A field consistent two-node curved axisymmetric shell element.
21. A. Tessler and L. Spiridigliozzi 1988 *International Journal for Numerical Methods in Engineering* **26**, 1071–1086. Resolving membrane and shear locking phenomena in curved shear-deformable axisymmetric shell elements.
22. A. K. Noor and J. M. Peters 1987 *Journal of the Engineering Mechanics Division*, *ASCE* **113**, 49–65. Analysis of laminated anisotropic shells of revolution.
23. A. K. Noor and J. M. Peters 1987 *Computer Methods in Applied Mechanics and Engineering* **61**, 277–301. Vibration analysis of laminated anisotropic shells of revolution.
24. A. K. Noor and J. M. Peters 1988 *International Journal for Numerical Methods in Engineering* **26**, 1145–1167. Stress and vibration analyses of laminated anisotropic shells of revolution.
25. S. C. Panda and R. Natarajan 1981 *Computers and Structures* **14**, 225–230. Analysis of laminated composite shell structures by finite element method.
26. A. Tessler and S. B. Dong 1981 *Computers and Structures* **14**, 335–344. On a hierarchy of conforming Timoshenko beam elements.
27. T. Kosawada, K. Suzuki and S. Takahashi 1985 *Bulletin of Japanese Society of Mechanical Engineers* **28**, 2041–2047. Free vibrations of toroidal shells.
28. T. Kosawada, K. Suzuki and S. Takahashi 1986 *Bulletin of Japanese Society of Mechanical Engineers* **29**, 3036–3042. Free vibrations of thick toroidal shells.